EXPERIMENTAL AND NUMERICAL ANALYSIS OF HIGH-CAPACITY SHEAR WALLS WITH MULTIPLE ROWS OF NAILS

Ruite Qiang[1], Lina Zhou[2], Chun Ni[3]

ABSTRACT: With the increase of building height in light wood-frame construction and seismic design spectra in the 2015 edition of National Building Code of Canada, stronger shear wall systems have been facing higher demands, especially for mid-rise wood-frame buildings located in high seismic zones. In collaboration with FPInnovations, a new high-capacity shear wall system with two and three rows of nails was developed. A total of 30 shear walls had been tested under reversed cyclic loading. Results showed that the lateral resistance of shear walls with multiple rows of nails is roughly proportional to the number of rows compared to a standard shear wall with the same sheathing thickness, nail diameter and nail spacing. However, new failure modes, such as splitting of bottom plates, out-of-plane separation of end studs from bottom plates, rupture of sheathing panels, etc. have limited the post-peak deformation of the high-capacity shear wall and its ductility. A better understanding on the stress-strain development of wood material and connections is needed to develop design details to prevent these failure modes and increase the ductility and design resistance of wood shear walls with multiple rows of nails. A preliminary 3D numerical model of high-capacity shear walls with multiple rows of nails were developed using ABAQUS to simulate the lateral performance and failure modes of high-capacity shear walls. Testing data from previous research by the authors was used to verify the modeling techniques developed in this study. Results show that the detailed 3D shear wall model can reasonably simulate the lateral resistance of high-capacity shear walls and the failure modes that are not common in regular shear walls.

KEYWORDS: high-capacity shear wall, multiple rows of nails, lateral load, numerical modelling

1 INTRODUCTION

Light wood frame shear wall systems have been widely used in the construction of multi-story residential and commercial wood buildings in North America. Consisting of wood framing members, wood-based sheathing panels and fasteners, wood frame shear walls are the main vertical component in resisting lateral loads caused by wind or seismic actions.

The height limit of wood frame buildings has been firstly increased from 4 to 6 stories since 2009 in BC, and the seismic design spectra have also been increased substantially for all site classes in the provincial and national building codes of Canada (NBCC) [1,2]. Therefore, the demand for higher lateral load resisting systems for mid-rise wood frame buildings has increased, especially in high seismic zones. To respond to this demand, a high-capacity shear wall system with multiple rows of nails along sheathing edges has been jointly developed by FPInnovations and University of Victoria. There were 30 high-capacity shear walls with two and three rows of nails along sheathing edges tested over a three-year period [3,4]. Results showed that the lateral resistance of shear wall with multiple rows of nails is almost proportional to the number of rows. However, new failure modes that are not common in standard shear walls were observed in high-capacity shear walls, such as splitting of bottom plates, out-of-plane separation of end studs from bottom plates, rupture of sheathing panels, etc. Present of these new failure modes limited the post-peak deformation of the high-capacity shear wall system and its ductility. Additional design details had been tried in the past few years to prevent these new failure modes. For example, double bottom plates were used to avoid splitting of bottom plates. However, reinforcing one element of the wall system may shift the weakest point to another location. A better understanding on the stress-stain development of sheathing panels, framing members and connections is needed to develop design details to prevent these undesirable brittle failures and increase the ductility and design resistance of wood shear walls with multiple rows of nails.

Numerical models of light wood frame shear walls have been developed with different methods in the past [4].

[1] Ruite Qiang, Department of Civil Engineering,
University of Victoria, Victoria BC, Canada, ruiteqiang@uvic.ca
[2] Lina Zhou, Department of Civil Engineering,
University of Victoria, Victoria BC, Canada, linazhou@uvic.ca
[3] Chun Ni, Advanced Building Systems, FPInnovations,
Vancouver BC, Canada, Chun.Ni@fpinnovations.ca

https://doi.org/10.52202/069179-0360

Different approaches were used to describe the monotonic and reversed-cyclic behavior of nail joints and shear walls in light wood frame buildings [5–8]. For shear wall models, framing members and sheathing panels are usually defined as elastic beam-type and shell-type element, respectively, while the sheathing-to-framing nail joints are represented by nonlinear link elements [9–12]. In a standard shear wall, the wall performance is mainly governed by sheathing-to-framing nail joints. The assumption of elastic behavior of framing members and sheathing panels, and pin connections between studs and plates, is usually acceptable. However, for high-capacity shear walls, in order to simulate the framing septation, wood splitting, sheathing rupture, etc. more realistic framing member connection performance and wood material damage should be considered in the model.

The objective of this study is to develop a detailed 3D shear wall model to predict the structural performance of high-capacity shear walls and simulate the failure modes including those that are not common in regular shear walls. The numerical models of high-capacity shear walls with three rows of nails were verified with the test results obtained in previous research by the authors [4]. Detailed wall components and boundary conditions were included in the model to regenerate the lateral behavior and failure modes of high-capacity shear walls tested in the lab. The modelling will provide insights for design and future testing of high-capacity shear walls.

2 EXPERIMENTAL STUDY

2.1 SHEAR WALL SPECIMEN AND TEST SETUP

There have been 30 high-capacity shear walls with two or three rows of nails along sheathing edges and reference walls tested in the past three years. Table 1 summarizes the details of the 22 shear walls tested in the first two years [3,4]. The wall details cover a combination of different sheathing panel thicknesses, nail sizes and nail spacings. For each configuration except the 9.5 mm panel thickness walls, a standard shear wall with one row of nails was also tested as reference. The shear wall specimens are 2.4 m × 2.4 m in dimension, constructed with 2 × 4 or 2 × 6 Douglas Fir dimension lumber, and vertically sheathed with 1.2 m × 2.4 m OSB panels on one side. Figure 1 shows the configuration of a shear wall specimen with three rows of nails.

Construction details and test set up of shear walls with three rows of nails are presented in this section as the numerical modelling described in this paper was based on shear walls with three rows of nails which are more prone to fail in the new failure modes.

The framing members were connected using F1667 NLCMMS69 (76.2 mm × 3.05 mm) power driven common nails. There were two rows of nails spaced at 200 mm on center for built-up end studs, built-up interior end studs, and top and bottom plates. For built-up center studs, three rows of nails (76.2 mm × 3.05 mm) spaced at 100 mm were used to prevent separation of center studs [4].

The shear wall specimens were fabricated and installed according to ASTM E2126 [13]. Figure 2 shows the schematic test set up. For all shear wall specimens, continuous 28.6 mm (1-1/8 in.) diameter tie-rods were used to resist overturning moment. 6 Hex A325 anchor bolts (22.2 mm in diameter) with steel bearing plates (127 mm in length × 127 mm in width × 6 mm in thickness) were used to connect both top and bottom plates to load spreader beam (C180 × 18) and foundation steel beam, respectively. Steel bearing plates (165 mm in length × 114 mm in width × 25 mm in thickness) were used to hold the tie-rod against the top plates (Fig. 2 B-B). The lateral load was applied through the steel load spreader beam to the top of the shear wall, as shown in Figure 2a. There was no vertical load applied on the wall specimens. Reversed cyclic loading was applied on tested specimens, following the CUREE protocol (method C) in ASTM E2126 [13].

Table 1: *Shear wall test configurations*

Wall #	OSB thickness (mm)	Nail size (mm)	Row of nails	Nail spacing along panel edges (mm)
1	9.5	63.5 × 3.33	2	100
2	9.5	63.5 × 3.33	2	75
3	11	63.5 × 3.33	3	100
4	11	63.5 × 3.33	3	75
4r	11	63.5 × 3.33	1	75
5	15	76 × 3.76	2	100
6	15	76 × 3.76	2	75
6r	15	76 × 3.76	1	75
7	15	76 × 3.76	3	100
8	15	76 × 3.76	3	75
8r	15	76 × 3.76	1	75

Note: "r" refers to regular shear walls with one row of nails along sheathing edges.

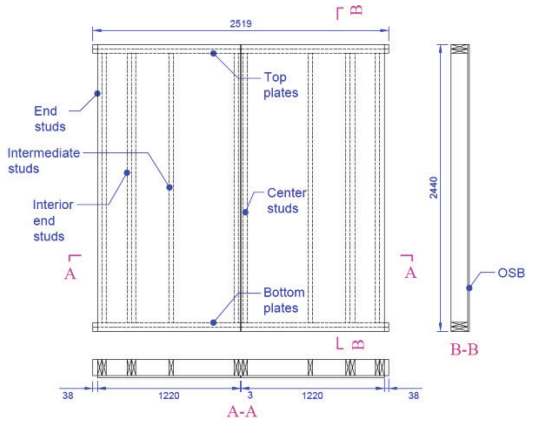

Figure 1*: Shear wall with three rows of nails [4] (Unit: mm)*

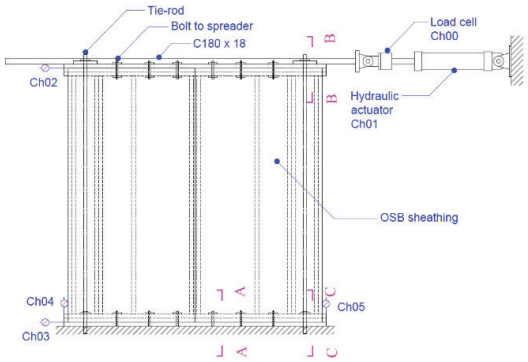

https://doi.org/10.52202/069179-0360

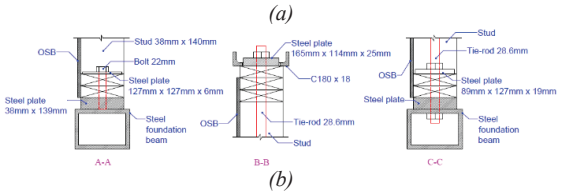

Figure 2: *Schematic of shear wall test set up: (a) front view, (b) cross section view [4]*

2.2 TEST RESULTS

Test results showed that shear walls with two rows of nails have approximately 2 times the lateral load resistance and energy dissipation capacity of a standard shear wall with the same sheathing thickness, nail diameter and nail spacing. According to seismic equivalency requirement in ASTMD7989 [14], a design value of 1.8 times standard shear walls can be assigned to shear walls with two rows of nails [3].

In general, shear walls with three rows of nails achieved approximately 3 times the lateral load resistance and energy dissipation capacity of a standard shear wall with the same sheathing thickness, nail diameter and nail spacing. However, a design value much less than three times of standard shear walls must be used to meet the ductility requirements. This is due to the undesirable failure modes which caused shear walls to lose resistance rapidly after the peak point [4].

Figure 3 shows the load-displacement response of walls with three rows of nails compared to a standard shear wall with one row of nails.

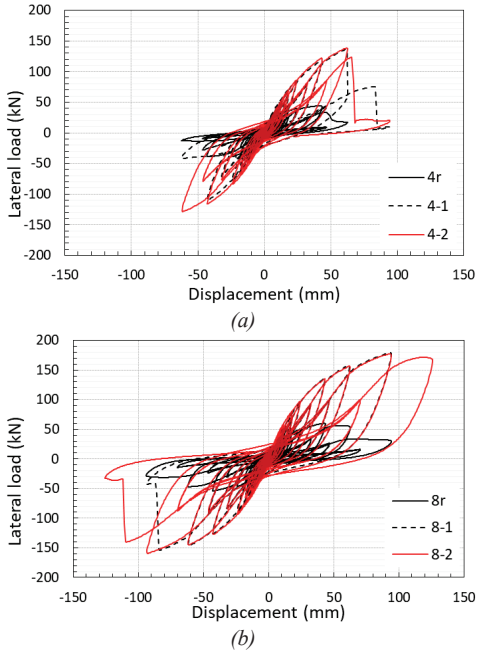

Figure 3: *Comparison of hysteresis loops of (a) Wall 4r, Wall 4-1, Wall 4-2, (b) Wall 8r, Wall 8-1, Wall 8-2*

2.3 FAILURE MODES

Besides common failure modes such as nail head pull through sheathing, nail chip-out from sheathing edge, nail withdrawal and fracture, other failure modes were also observed in the testing of high-capacity shear walls, including bottom plate splitting, end stud pull-out from bottom plates, center stud separation, and sheathing rupture.

In Wall 3 and Wall 4 (Table 1), bottom plates split due to a combination of factors (Figure 4 a), such as increased uplift force from three rows of nails, while the end of bottom plates was not restrained from uplifting. The splitting of bottom plates is brittle and undesired. This failure mode was prevented after installing bearing plates on bottom plates where tie-rods were located.

For most of the shear wall specimens with three rows of nails, end studs were separated from bottom plates (Figure 4 b), which led to the rupture of the sheathing panels in some cases (Figure 4 c). This is because the shear walls were only sheathed on one side which caused an out-of-plane moment on the end studs. This moment was amplified with increase of the number of rows of nails and using of 2 × 6 lumber compared to a 2 × 4 standard wall. The nails that connect bottom plates to end studs were not able to hold end studs and bottom plates together. The failure mode of end stud separation is brittle and need to be prevented.

Sheathing rupture was also observed in one of the shear walls (Figure 4 d). To prevent such failure, sheathing panels with higher thickness should be used.

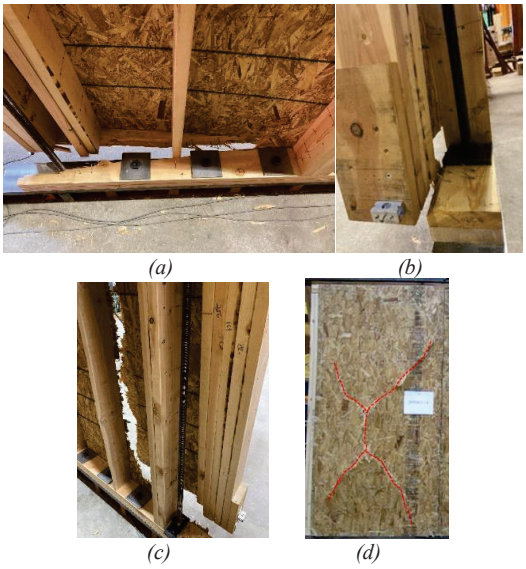

Figure 4: *Failure modes: (a) Splitting of bottom plates, (b) Separation of end studs, (c) Sheathing rupture due to end stud separation, (d) Sheathing rupture due to buckling and tension [4]*

2.4 NAIL JOINT TESTS

Nail joints made from the same materials (dimension lumber, OSB panels, and nails) as shear walls with two rows of nails were tested [3]. The test results were used in

the modelling of shear walls. Nail size of 63.5 mm × 3.33 mm and 76 mm × 3.76 mm were combined with sheathing thickness of 15 mm (Table 2). Figure 5 shows the test setup and configurations of the nail joint. The reversed cyclic loading protocol (CUREE) used for shear wall testing were adopted for nail joint testing, with half the displacement amplitude.

Table 2 shows the details of nail joint configurations and the average peak resistance of all replicates. It was found that the tested peak resistance of nail joints for both nail sizes is approximately 1.7 times the design value based on CSA O86 [15].

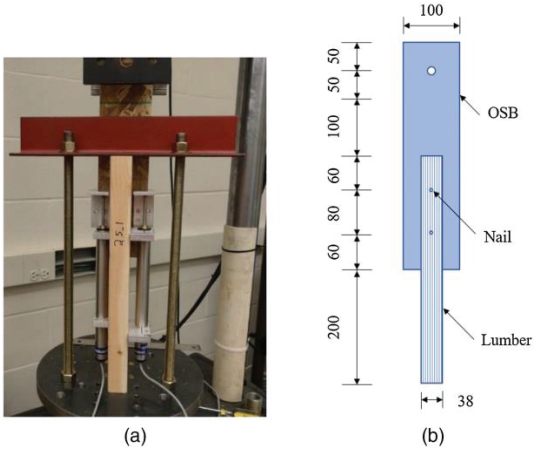

Figure 5: *Nail joint test: (a) Test set up, (b) Specimen dimension (mm) [3]*

Table 2: *Configuration and test results of the nail joints[3]*

Nail joint #	OSB thickness (mm)	Nail size (mm)	Peak resistance[1] (N)	Design resistance (N)
N2.5	15	63.5 × 3.33	1619	954
N3	15	76 × 3.76	1835	1105

1. The peak resistance is based on nail joint with one nail.

3 NUMERICAL MODELLING

Numerical models of the shear walls with three rows of nails were developed in ABAQUS. The sheathing-to-framing and framing-to-framing nail joints were simulated by a nonlinear fastener (link) element. The nail joint test data was used to derive the properties of fastener elements through fitting the load-displacement curve to the test curve. These properties of fasteners were then implemented in the shear wall models.

3.1 NAIL JOINT ELEMENT PROPERTIES

The tested nail joints with 15 mm sheathing thickness and 63.5 mm × 3.33 mm and 76.2 mm × 3.76 mm nails were modeled. The two nails connecting OSB panel and lumber were modelled using mesh independent fasteners. The fastener properties were derived from the average backbone curves and its corresponding EEEP parameters [13].

The fastener elements in ABAQUS were used to define a point-to-point connection between surfaces of OSB panel and lumber. An influence radius equal to the diameter of nail shank was used for each type of nails. A connector section was assigned to the fastener element, which allows behavior in three local directions. Elastic, plastic and damage behavior were assigned in the connector section. For elastic behavior, spring stiffness was assigned for each local direction. The average secant stiffness, *D*, derived from the tested nail joints was used, as shown in Table 3. Coupled plastic behavior with nonlinear isotropic hardening was defined using exponential law as shown in the following Equation (1):

$$F_0 = F|_0 + Q_{inf}\left(1 - e^{-b\bar{u}^{pl}}\right) \quad (1)$$

where F_0 is the yield surface size defined as the equivalent force in the connector, $F|_0$ is the yield force at zero plastic motion, Q_{inf} is the maximum change of yield surface, $\bar{u}^{pl}$ is the relative plastic motion, b is the rate of the change of the yield surface. The relative motion components are coupled in a quadratic form by defining the potential function [16]. Coupled damage behavior was also defined based on relative plastic motion, where linear softening was assumed.

The parameters for plastic and damage behavior were derived from the average backbone curve of the tests, as shown in Figure 6. Table 4 summarizes the properties of the fasteners, in which b is modified after back calculated from test data using Equation (1), plastic motion at failure was modified based on actual failure displacement to fit the test curve.

Monotonic push-over displacement was applied in the modeled nail joint. Load-displacement relationship of the models is compared with the average backbone curve of the tested nail joints, as shown in Figure 7. Overall, the parameters listed in Table 4 give a good fitting of the performance of the nail joints to the test data and can capture the post peak load-displacement behavior.

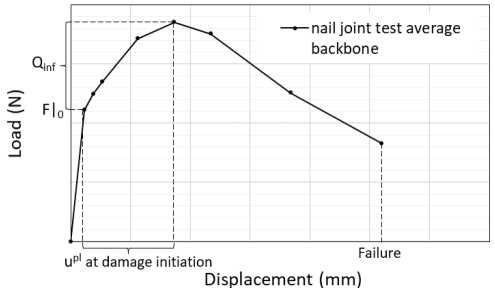

Figure 6: *Plastic and damage parameters from tested backbone curve*

Table 3: *Properties of fastener element for nail joints*

Connector property	Nail size (mm)	
	63.5 × 3.33	76 × 3.76
D (N/mm)	827.5	980.6
$F\|_0$ (N)	964.8	1100.1
Q_{inf} (N)	607.9	743.1
b	0.4	0.4
Plastic motion at damage initiation (mm)	7.6	7.5
Plastic motion at failure (mm)	30	30

https://doi.org/10.52202/069179-0360

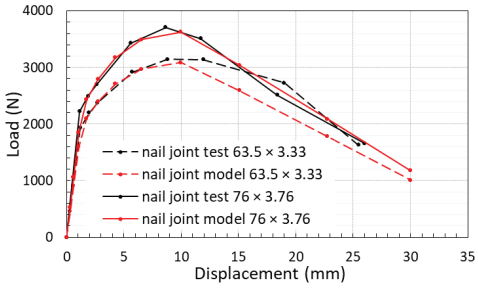

***Figure 7:**. Comparison of load displacement curves between nail joint tests and models*

3.2 SHEAR WALL MODEL

In the shear wall model, more details of the shear wall are included to simulate both the overall load displacement behavior and the possible new failure modes.

The framing members were represented with solid elements (C3D8R), and sheathings panels were modelled with continuum shell elements (CS8R). The framing members and sheathing were both assumed to be elastic. Table 3 summarizes the elastic properties of Douglas fir lumber and OSB panel. Sheathing-to-framing nails, nails for built-up studs and plates, nails connecting studs to plates were all represented by the fastener elements, in which both shear and withdrawal components were included. For sheathing-to-framing nails, properties are derived from nail joint fitting process (Table 3). Since properties in Table 3 refers to 15 mm sheathing thickness, a factor of 0.89 was used to adjust the resistance for 11 mm sheathing panel with combination of 63.5 mm × 3.33 mm nails based on the ratio of design resistance of these two different nail joints in O86-19 [15]. For nail joints in built-up studs and plates (76.2 mm × 3.05 mm), a factor of 0.98 was applied to the properties of 63.5 mm × 3.33 mm nail joint in Table 3. For nails connecting studs to top and bottom plates, an end grain factor of 0.67 was applied to the nail joints for built-up members to further reduce the resistance [15]. Table 5 and Table 6 shows the modified connector properties used for sheathing panels and framing nails.

***Table 4:** Material properties of nail joint model*

Material property	Douglas-Fir[1] (Mpa)	OSB[2] (Mpa)
E_1	11000	5323
E_2	748	3231
E_3	550	-
G_{12}	704	1574
G_{13}	758	1574
G_{23}	77	1574
μ_{12}	0.29	0.31
μ_{13}	0.45	-
μ_{23}	0.39	-

1. Properties of Douglas-Fir are obtained from O86 and Wood Handbook [15,17].
2. Properties of OSB are obtained from studies of Islam et al. [18].

***Table 5:** Properties of fastener elements used for sheathing-to-framing nails*

Connector property	Nail size (mm)	
	63.5 × 3.33	76 × 3.76
D_{11} (N/mm)	734.3	980.6
D_{22} (N/mm)	734.3	980.6
D_{33}[1] (N/mm)	9.6	10.6
$F\|_0$ (N)	856.1	1100.1
Q_{inf} (N)	539.4	743.1
b	0.4	0.4
Plastic motion at damage initiation (mm)	7.6	7.5
Plastic motion at failure (mm)	30	30

1. D_{33} is the nail withdrawal stiffness of sheathing-to-framing nails based on the local coordinate, which was assumed to be a small percentage of the lateral stiffness in this preliminary modeling with the assumption that the withdrawal resistance is limited after yielding of nails in shear and losing of friction from the surrounding wood when the nail is pulling out from studs.

***Table 6:** Properties of fastener element used in framing members*

Connector property	Nail type	
	Built-up member	Stud to plate
D_{11} (N/mm)	811.5	543.7
D_{22}[1] (N/mm)	811.5	543.7
D_{33} (N/mm)	811.5	543.7
$F\|_0$ (N)	946.0	633.8
Q_{inf} (N)	596.1	399.4
b	0.4	0.4
Plastic motion at damage initiation (mm)	7.6	7.6
Plastic motion at failure (mm)	30	30

1. D_{22} is the nail withdrawal stiffness of built-up members and stud-to-plate connections based on the local coordinates. No reduction of the lateral stiffness was used in this preliminary model.

Figure 8 shows a shear wall model. The assembly includes the shear wall panel, steel loading beam and foundation beam. The fastener elements were assigned for all built-up studs, top and bottom plates, stud-to-plates connections, and sheathing-to-framing connections. The top and bottom plates have pre-dill holes representing locations of anchor bolts and hold-downs (tie-rods). The hold-downs were represented by axial connector elements with a stiffness of 42.34 kN/mm [19], where the top of the hold-down element was coupled with the top plates over a surface area of the same size of the bearing plates. The bottom of the hold-down element was fixed at the foundation. The bottom plates were anchored to the foundation beam at the surfaces of the same size of bearing plates. The top plates and loading beam are simplified as tie constrained to eliminate slip between top plates and loading beam. A monotonic lateral displacement is applied through the loading beam. There's no out-of-plane degree of freedom allowed on the loading beam.

https://doi.org/10.52202/069179-0360

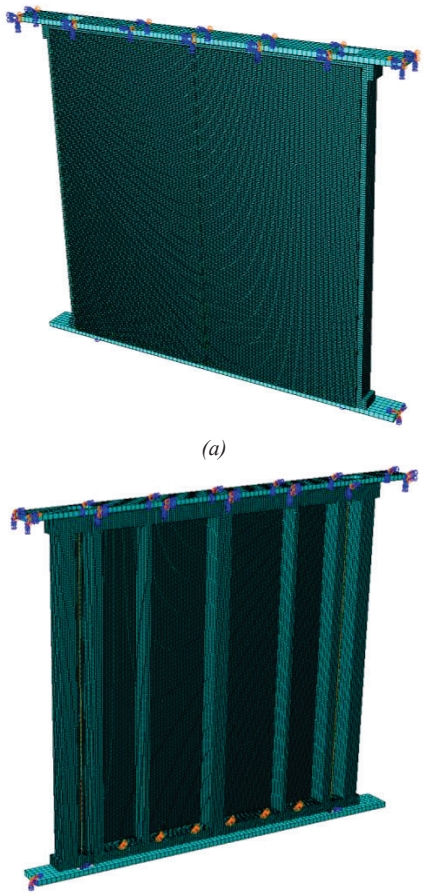

(a)

(b)

Figure 8: *Shear wall model: (a) Front view, (b) Back view*

The load-displacement curves of the models are compared with the hysteresis loops of the tests. There are in total 6 wall configurations (Wall 3, 4, 4r, 7, 8, 8r in Table 2) modelled, including two reference wall models. The results are shown in Figure 9.

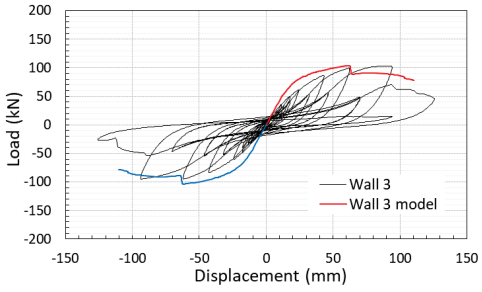

(a)

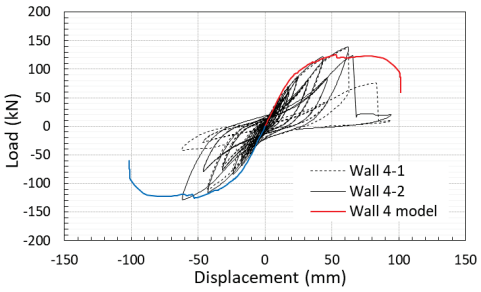

(b)

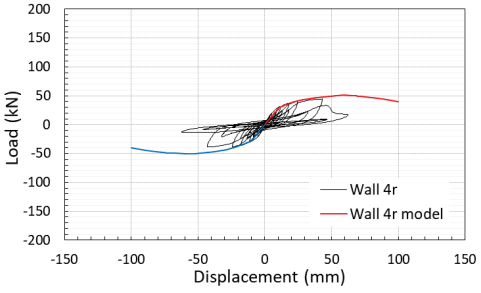

(c)

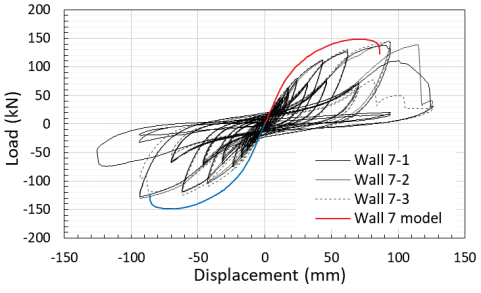

(d)

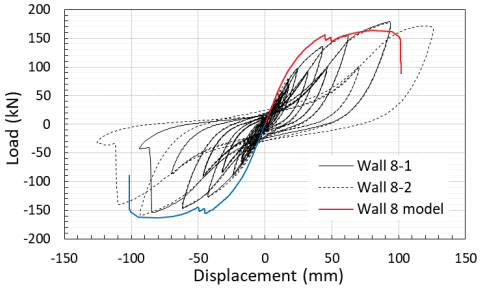

(e)

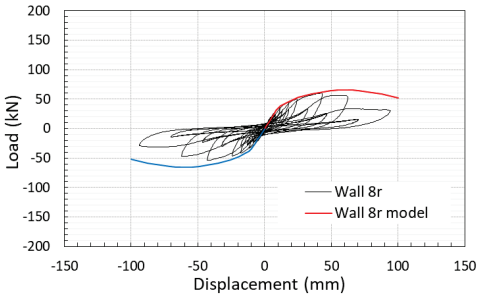

(f)

Figure 9: *Comparison between model and test results: a) Wall 3, (b) Wall 4, (c) Wall 4r, (d) Wall 7, (e)Wall 8, (f) Wall 8r*

Overall, the model can predict the nonlinear behavior of

https://doi.org/10.52202/069179-0360

the shear wall including the post-peak load drop. The peak resistance of models and test results are compared in Table 7. It can be seen that the discrepancy of peak load is with 10% for most cases. In all shear walls with three rows of nails, namely Wall 3, Wall 4, Wall 7 and Wall 8, the stiffness of the models appears to be higher than the tested shear walls (Figure 9 a, b, d, e). In the reference shear walls, namely Wall 4r and Wall 8r, the models reach their peak load at a larger displacement than the tested walls, and the models do not have a significant load drop after peak load (Figure 9 c, f).

Table 7: *Comparison of the tested peak resistance and model peak resistance*

Wall #	Test P_{peak} (kN)	Model P_{peak} (kN)	Model peak/Test peak
3	91.5	103.5	1.1
4-1	114.1	125.5	1.1
4-2	133.7	125.5	0.9
4r	41.7	50.7	1.2
7-1	132.1	148.6	1.1
7-2	137.6	148.6	1.1
7-3	131.2	148.6	1.1
8-1	166.7	155.7	0.9
8-2	168.4	155.7	0.9
8r	57.2	65.7	1.1

In the shear wall models with three rows of nails, end stud separation from bottom plates was observed, as shown in Figure 10 a, which caused the load drop at the end of the load-displacement curves in Wall 4, Wall 7 and Wall 8. The end studs on the opposite side of the wall have also separated slightly from the top plates (Figure 10 b). The separation of end studs is due to the eccentric moment on end studs caused by sheathing only on one side of the wall and the relatively low resistance of fasteners connecting the end studs to the bottom and top plates, which are not strong enough to counteract the out-of-plane moment. The failure modes were also observed in shear wall tests. Separation of end stud from bottom and top plate can be prevented through reinforcing the stud-to-plate connections.

As framing members and sheathing panels were assumed to be linear elastic in this preliminary model to reduce convergence difficulty, the failure modes such as bottom plate splitting and sheathing rupture was not captured. Figure 11 shows the axil stress on framing elements. It can be seen that the compression stress was concentrated on end studs which indicates that the compression force due to over-turning moment is mainly resisted by the end studs. The contribution from the interior end studs (Figure 1) is limited. Therefore, when tie-rods are used in shear walls as hold-downs, the interior studs should neither be counted for resisting the compression force due to over-turning, nor the bearing area of the bottom plates. Figure 12 shows the principal stress distributed on the sheathing panels before end stud separation. It can be seen that the principal tensile and compressive stress developed on the sheathing panels are diagonal, which explains the failure in one of the Wall 4 replicates tested, in which 'X' shape fracture occurred in one of the sheathing panels (Figure 4 d).

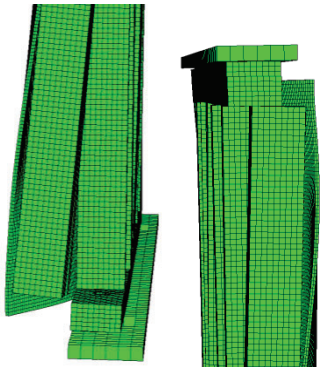

(a) (b)

Figure 10: *Failure of the shear wall model (Wall 4): (a) End stud separation from bottom plates, (b) End stud separation from top plates*

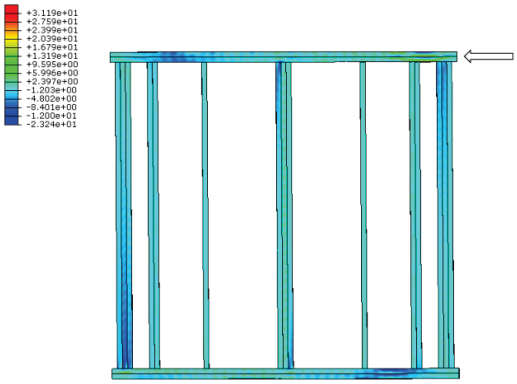

Figure 11: *Stress S11 along grain direction of framing members in Wall 4 model(MPa)*

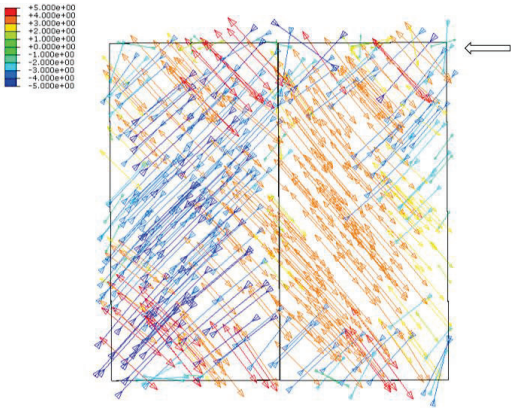

Figure 12: *Principal Tensile and compressive stress in sheathing panels of shear wall model (Wall 4) before end stud separation (MPa)*

Overall, the models can generally predict the load-displacement behavior and the end stud separation in walls with three rows of nails. With only fastener behavior assumed to be non-linear, the models are not able to predict material failure in sheathing panels and framing members. Although the stress distribution in sheathings showed potential cause for sheathing rupture, additional

wood damage definition is needed to simulate those failure modes.

3.3 ON-GOING WORKS

To better understand the split of bottom plate of shear walls with multiple rows of nails, a more detailed 3D sub-model of the shear wall is being developed only including the bottom plates and foundation beam. Steel anchor bolts and bearing plates are installed in the bottom plates. Nails and initial imperfections (cracks, checking) on wood will be added (Figure 13). The objective of this modeling is to capture the crack propagation parallel to grain under the one-sided shear force on the bottom plate. Moreover, more detailed material definition will be included in the shear wall model to capture the fracture of sheathing panel due to buckling or tension.

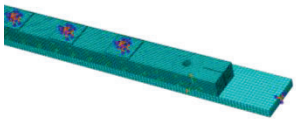

Figure 13: *Detailed sub-model of bottom plates*

4 CONCLUSIONS

In this study, high-capacity shear walls with multiple rows of nails were introduced and numerically simulated using ABAQUS. Test results of shear walls with two and three rows of nails were presented. The lateral load resistance is proportional to number of rows of nails. Failure modes that are not commonly observed in regular shear walls were found in shear walls with multiple rows of nails. To study the behavior of high-capacity shear walls, a preliminary 3D shear wall model with three rows of nails was developed. Fastener elements were used to simulate the non-linear behavior of nails, firstly, the properties for fastener elements were derived from the nail joint tests and through a fitting process. The fastener properties were then implemented in the shear wall models. In the shear wall model, all the framing-to-framing and framing-to-sheathing nails were represented by the non-linear fastener elements, while framing members and sheathing panels were assumed to be linear elastic. Components such as anchors, hold-downs, foundation beam and loading beam were also included. The main findings of the numerical modeling analysis are summarized as follows:

- The preliminary 3D model developed in this study can well capture the load-displacement performance of the high-capacity shear walls with multiple rows of nails, and predict the end-stud separation from the bottom plate.
- Failure on sheathing and framing members cannot be captured by the current preliminary model due to linear elastic material assumption.
- The principal stress developed on sheathing panels is diagonal, which explains the “X” shape fracture observed in one of the wall panels in the test.
- Compression force due to over-turning moment is mainly resisted by the end studs. The interior end studs should neither be counted for resisting this compression force in design, nor the bearing area of the bottom plates in a shear wall when tie-rods are used as hold-downs.

More detailed modelling and material damage definition need to be added to the current model to study the splitting of bottom plates, sheathing panel fracture, and other failure modes of high-capacity shear walls.

ACKNOWLEDGEMENT

This project is funded by Canadian Forest Service of Natural Resources Canada and Forestry Innovation Investment Ltd. in BC – Wood First Program. Donation of continuous threaded steel rods, coupler nuts and nuts by Simpson-Strong Tie, which have been used for tie-downs of the shear wall specimens, is greatly appreciated.

REFERENCE

[1] Canadian Commission on Building and Fire Codes. National Building Code of Canada: 2020 2020.

[2] Canadian Commission on Building and Fire Codes. National Building Code of Canada 2015. https://doi.org/10.4224/40002005.

[3] Derakhshan SS, Ni C, Zhou L, Qiang R, Huang D. Cyclic test and seismic equivalency evaluation of high-capacity light wood-frame shear walls for midrise buildings. J Struct Eng, 148: 4022168, 2022.

[4] Qiang R, Zhou L, Ni C, Huang D. Seismic performance of high-capacity light wood frame shear walls with three rows of nails. Eng Struct, 268:114767,2022. https://doi.org/10.1016/j.engstruct.2022.114767.

[5] Ayoub A. Seismic analysis of wood building structures. Eng Struct, 29:213–23, 2007. https://doi.org/10.1016/j.engstruct.2006.04.011.

[6] Boudaud C, Humbert J, Baroth J, Hameury S, Daudeville L. Joints and wood shear walls modelling II: Experimental tests and FE models under seismic loading. Eng Struct,101:743–9, 2015. https://doi.org/10.1016/j.engstruct.2014.10.053.

[7] Humbert J, Boudaud C, Baroth J, Hameury S, Daudeville L. Joints and wood shear walls modelling I: Constitutive law, experimental tests and FE model under quasi-static loading. Eng Struct;65:52–61,2014. https://doi.org/10.1016/j.engstruct.2014.01.047.

[8] Pang WC, Rosowsky D V., Pei S, Van De Lindt JW. Evolutionary parameter hysteretic model for wood shearwalls. J Struct Eng,133(8):1118–29, 2007. https://doi.org/10.1061/(asce)0733-9445(2007)133:8(1118).

[9] Xu J, Dolan JD. Development of nailed wood joint element in ABAQUS. J Struct Eng, 135:968–76,2009. https://doi.org/10.1061/(asce)st.1943-

https://doi.org/10.52202/069179-0360

541x.0000030.
[10] Peng C, El Damatty AA, Musa A, Hamada A. Simplified numerical approach for the lateral load analysis of light-frame wood shear wall structures. Eng Struct, 219:110921, 2020. https://doi.org/10.1016/j.engstruct.2020.110921.
[11] Collins M, Kasal B, Paevere P, Foliente GC. Three-dimensional model of light frame wood buildings. II: Experimental investigation and validation of analytical model. J Struct Eng, 131:684–92,2005. https://doi.org/10.1061/(asce)0733-9445(2005)131:4(684).
[12] Gattesco N, Boem I. Stress distribution among sheathing-to-frame nails of timber shear walls related to different base connections: Experimental tests and numerical modelling. Constr Build Mater, 122:149–62, 2016. https://doi.org/10.1016/j.conbuildmat.2016.06.079.
[13] ASTM - American Society for Testing and Materials. E2126 - Standard Test Methods for Cyclic (Reversed) Load Test for Shear Resistance of Vertical Elements of the Lateral Force Resisting Systems for Buildings, i:1–14, 2019. https://doi.org/10.1520/E2126.
[14] ASTM - American Society for Testing and Materials. D7989 - Standard Practice for Demonstrating Equivalent In-Plane Lateral Seismic Performance to Wood-Frame Shear Walls Sheathed with Wood Structural Panels, i:1–9, 2018. https://doi.org/10.1520/D7989-18.
[15] Canadian Standards Association. CAN/CSA-086:19. Engineering design in wood, 1, 2019.
[16] Abaqus 6.14 Analysis User's Guide. Dassault Systèmes 2014.
[17] Forest Products Laboratory. Wood handbook : wood as an engineering material. 1999. https://doi.org/10.2737/FPL-GTR-113.
[18] Shahidul Islam M, Islam MN, Shahria Alam M. Properties of oriented strand board (OSB), and timber to evaluate the stiffness of timber L-joist. 6th Int Conf Eng Mech Mater 2017, 2:790–801, 2017.
[19] Simpson Strong-Tie Company Inc. Strong-Rod™ Systems Seismic and Wind Anchor Tiedown System Guide 2022.